



HAL
open science

Genetic algorithm and Monte Carlo simulation for a stochastic capacitated disassembly lot-sizing problem under random lead times

Ilhem Slama, Oussama Ben-Ammar, Alexandre Dolgui, Faouzi Masmoudi

► To cite this version:

Ilhem Slama, Oussama Ben-Ammar, Alexandre Dolgui, Faouzi Masmoudi. Genetic algorithm and Monte Carlo simulation for a stochastic capacitated disassembly lot-sizing problem under random lead times. *Computers & Industrial Engineering*, 2021, pp.107468. 10.1016/j.cie.2021.107468. hal-03258442

HAL Id: hal-03258442

<https://hal.science/hal-03258442v1>

Submitted on 2 Aug 2023

HAL is a multi-disciplinary open access archive for the deposit and dissemination of scientific research documents, whether they are published or not. The documents may come from teaching and research institutions in France or abroad, or from public or private research centers.

L'archive ouverte pluridisciplinaire **HAL**, est destinée au dépôt et à la diffusion de documents scientifiques de niveau recherche, publiés ou non, émanant des établissements d'enseignement et de recherche français ou étrangers, des laboratoires publics ou privés.



Distributed under a Creative Commons Attribution - NonCommercial 4.0 International License

Genetic algorithm and Monte Carlo simulation for a stochastic capacitated disassembly lot-sizing problem under random lead times

Ilhem Slama^{a,*}, Oussama Ben-Ammar^b, Alexandre Dolgui^a, Faouzi Masmoudi^c

^a*IMT Atlantique, LS2N-CNRS, La Chantrerie, 4 rue Alfred Kastler - B.P. 20722, 44307 Nantes, France*
{ilhem.slama;alexandre.dolgui}@imt-atlantique.fr

^b*Mines Saint-Étienne, Univ. Clermont Auvergne, UMR-CNRS 6158 LIMOS, CMP Department of Manufacturing Sciences and Logistics, 880 route de Mimet, F-13541 Gardanne, France*
oussama.ben-ammam@emse.fr

^c*Engineering School of Sfax, Laboratory of Mechanic, Modeling and Production (LA2MP), University of Sfax, Tunisia*
masmoudi.fawzi@gmail.com

*Corresponding author
Email address: ilhems1m.fsegs@gmail.com (Ilhem Slama)

Genetic algorithm and Monte Carlo simulation for a stochastic capacitated disassembly lot-sizing problem under random lead times

Abstract

The purpose of this research is to propose several optimization methods for the stochastic multi-period disassembly lot-sizing problem. The case of one type of end-of-life product and a two-level disassembly system is studied. The disassembly lead times are discrete random variables with a known and bounded probability distribution. The objective is to optimize the expected value of the total cost, which is the sum of setup cost, overload cost, inventory holding cost and backlogging cost. Three approaches were developed to solve the studied problem: (i) a two-stage mixed-integer linear programming model based on all possible scenarios for small instances, (ii) a sample average approximation approach based on Monte Carlo simulation for medium-scale instances and, (iii) an optimization approach based on the Monte Carlo simulation and a genetic algorithm for large-scale instances. Experimental results show the effectiveness of the proposed models which can be used to support decision-making on replenishment and disassembly plans.

Keywords: Capacitated disassembly lot-sizing, Stochastic lead times, Monte Carlo Simulation, Sample average approximation, Genetic algorithm.

1. Introduction

A great deal of attention is now being paid to dealing with end-of-life (EoL) products for economic and environmental reasons such as incineration sites and shortages of landfill sites, legislative pressure, economic considerations etc. In particular, much legislation imposes an obligation on the manufacturing industry to collect and recover EoL products in more environmentally conscious ways (Kim et al., 2018b).

The disassembly operation is one of the important activities in recycling raw materials and separating reusable components. It can be defined as the process of separating EoL products into multiple components by sorting and inspection operations. Various disassembly optimization problems have been intensively studied in the literature such as disassembly line balancing problems (e.g., Liu et al., 2020; Xu et al., 2020; Ren et al., 2020; Jeunet et al., 2019; Li et al., 2019; Tseng et al., 2019, 2018; Li et al., 2018; Zhang & Zhang, 2010; Agrawal & Tiwari, 2008; Efendigil et al., 2008; Tiwari, 2005; Dini et al., 2001; Güngör & Gupta, 2001; Gungor & Gupta, 1998), the disassembly sequencing problems (e.g., Liu et al., 2020; Xu et al., 2020; Ren et al., 2020; Li et al., 2019; Jeunet et al., 2019; Tseng et al., 2019, 2018; Li et al., 2018; Han et al., 2013; Zhang & Zhang, 2010; Efendigil et al., 2008; Rai et al., 2002; Dini et al., 2001; Gungor & Gupta, 1998), the disassembly lot-sizing problem (e.g., Pour-Massahian-Tafti et al., 2020a,b; Slama et al., 2020; Habibi et al.,

16 2019; Tian & Zhang, 2019; Piewthongngam et al., 2019; Ji et al., 2016; Prakash et al., 2012; Kim et al.,
17 2006a, 2003) and other interesting issues.

18 In this paper the demand for components must be satisfied from the disassembly of EoL products. The
19 objective is to optimize the disassembly plan under capacity constraint and uncertainty of disassembly lead
20 times (DLT). According to Ilgin & Gupta (2010), the studied problem enters the classification of the Dis-
21 assembly Lot Sizing Problem (DLSP) that optimizes disassembly processes in order to satisfy demand of
22 components over a given planning horizon.

23 Recently, a great deal of attention has been paid to studying disassembly lot-sizing problems. Many
24 researchers have developed stochastic and deterministic approaches to optimize the disassembly plan for
25 complex EoL products. Nevertheless, the majority of studied problems consider a deterministic environment
26 and neglect uncertainty. In practice, managing disassembly operations is difficult due to technical problems
27 (absenteeism, limited disassembly capacity, quality problem, etc.). When an EoL product is disassembled, it
28 is fundamental to ensure that the right model is applied. Owing to the complexity of the manual disassembly
29 operation, the workforce is often the major factor generating uncertainty regarding disassembly duration.
30 Consequently, this uncertainty of disassembly lead times (DLT) could disturb the whole disassembly line and
31 create additional costs related to inventory levels, tardiness penalties, lost sales, overload capacity, etc.

32 The aim of this paper is to optimize the basic two-level disassembly lot-sizing model under stochastic
33 DLT. The demand and available capacity are fixed and known in advance. The disassembly lead times are
34 discrete random variables that follow a known and bounded probability distribution. Here, we assume that
35 the disassembly plan is frozen over a given planning horizon of several periods. In this case, even if the lead
36 times are revealed as time goes by, the two-stage stochastic model remains valid. This is relevant in the
37 capacity planning decision, as the schedule of the employees' weekly work schedules cannot be modified at
38 short notice.

39 In this paper, we consider a predictive strategy and develop a two-stage model based on scenario approach.
40 In our two-stage decision process, the disassembly lead times for the entire time horizon are revealed once the
41 first stage decisions are made. These decisions correspond to the disassembly, ordering setup and disassembly
42 overtime decisions for each time period. The second stage involves inventory and backlog decisions. The
43 questions then become: At which point in time should we start the disassembly? and what quantity must
44 be disassembled?

45 We summarize below the contributions and innovations of this study:

- 46 1. An original stochastic Capacitated Disassembly Lot Sizing (CDLS) model is formulated as a two-Stage
47 Mixed Integer Linear Program (2S-MILP).
- 48 2. To alleviate the scalability issues, a sample average approximation approach (SAA) based on Monte
49 Carlo simulation is proposed.
- 50 3. A sensitivity study is introduced to analyze the effect of disassembly lead time variability on the
51 robustness of the proposed SAA algorithm.

52 4. To solve large scale problems, a model coupling MC simulation and a genetic algorithm (MC-GA) is
53 proposed.

54 5. Useful managerial implications for industry practitioners are provided.

55 The rest of this paper is organized as follows. The next section outlines a brief overview of the stochastic
56 DLSP literature. Section 3 gives the problem statement and model formulation. Section 4 presents the
57 approach based on sample average approximation algorithm. In section 5, we introduce the model coupling
58 MC simulation and a genetic algorithm. Section 6 reports numerical results. The paper ends with conclusions
59 and avenues for future studies.

60 2. Literature review

61 In the literature, the majority of work focused on DLSP in a deterministic environment. Concerning this
62 field, the existing literature can be split into two categories: (i) uncapacitated problems (see for example [Pour-](#)
63 [Massahian-Tafti et al., 2020a,b](#); [Godichaud & Amodeo, 2019](#); [Piewthongngam et al., 2019](#); [Kim et al., 2018a](#);
64 [Godichaud & Amodeo, 2018](#); [Kang et al., 2016](#); [Gupta & Lambert, 2016](#); [Prakash et al., 2012](#); [Kim et al.,](#)
65 [2009](#); [Langella, 2007](#); [Kim et al., 2006b](#); [Lee et al., 2004](#); [Lee & Xirouchakis, 2004](#); [Kim et al., 2003](#); [Neuendorf](#)
66 [et al., 2001](#); [Taleb et al., 1997a,b](#)) and (ii) capacitated ones (see for example [Slama et al., 2020](#); [Ji et al., 2016](#);
67 [Ullerich & Buscher, 2013](#); [Kim et al., 2006a, 2005](#); [Lee et al., 2002](#)). Table 1 gives a recapitulation of previous
68 works which we have classified as deterministic *vs* stochastic approaches. For more detailed literature reviews,
69 readers can refer to [Slama et al. \(2019\)](#) and [Kim et al. \(2007\)](#).

Table 1: Summary of relevant literature.

(a) Deterministic approaches.

Authors	Criteria	Resolution	BOM		Cap	PC
			T	M		
Gupta & Taleb (1994)	$Min(NP)$	R-MRP		✓		
Taleb et al. (1997a)	$Min(NP)$	R-MRP		✓		
Taleb et al. (1997b)	$Min(NP + D_c)$	heuristics		✓		
Neuendorf et al. (2001)	$Min(NP)$	Petri nets		✓		
Lee et al. (2002)	$Min(P_c + H_c + D_c)$	LP		✓	✓	
Kim et al. (2003)	$Min(S_c + H_c + D_c)$	LP		✓	✓	
Lee et al. (2004)	$Min(S_c + P_c + H_c + D_c)$	LP		✓		✓
Lee & Xirouchakis (2004)	$Min(S_c + P_c + H_c + D_c)$	Heuristic		✓		✓
Kim et al. (2005)	$Min(NP)$	DP		✓	✓	
Kim et al. (2006b)	$Min(S_c + H_c + D_c)$	Heuristic		✓	✓	
Kim et al. (2006a)	$Min(S_c + H_c + D_c)$	LH		✓	✓	
Kim et al. (2008)	$Min(S_c + H_c)$	DP	✓			
Gao & Chen (2008)	$Min(S_c + H_c + D_c)$	GA		✓		
Barba-Gutiérrez et al. (2008)	$Min(S_c + H_c + D_c)$	LS-RMRP		✓		
Kim et al. (2009)	$Min(S_c + H_c)$	Branch and bound		✓	✓	
Kim & Lee (2011)	$Min(S_c + H_c + D_c)$	Heuristic		✓		
Prakash et al. (2012)	$Min(H_c + D_c + P_c + S_c)$	CBSA		✓		✓
Ullerich & Buscher (2013)	$Min(H_c + D_c + P_c)$	Heuristic	✓			✓
Ji et al. (2016)	$Min(S_c + H_c + D_c + Z_c + C_c)$	LH	✓			✓
Godichaud et al. (2015)	$Min(S_c + H_c + L_c + O_c)$	GA	✓		✓	
Tian & Zhang (2019)	$Min(S_c + P_c + H_c + W_c)$	PSO	✓			
Kim et al. (2018a)	$Min(S_c + H_c + D_c)$	Heuristic		✓		
Godichaud & Amodeo (2018)	$Min(D_c + H_c + W_c + L_c)$	EOQ model	✓			
Piewthongngam et al. (2019)	$Min(S_c + H_c + D_c + Z_c)$	MILP		✓		✓
Godichaud & Amodeo (2019)	$Min(D_c + H_c + W_c + L_c)$	EOQ model		✓		
Slama et al. (2020)	Max profit	MIP		✓	✓	✓
Pour-Massahian-Tafti et al. (2020a)	Max profit	EOQ model	✓			
Pour-Massahian-Tafti et al. (2020b)	$Min(S_c + H_c + D_c)$	Heuristics	✓			✓

(b) Stochastic approaches.

Authors	Objective	Resolution	Uncertainty		
			Yield	Demand	DLT
Inderfurth & Langella (2006)	$Min(NP)$	Heuristic	✓		
Barba-Gutiérrez & Adenso-Díaz (2009)	$Min(NP)$	F-RMRP		✓	
Kim & Xirouchakis (2010)	$Min(S_c + H_c + L_c)$	LH		✓	
Fang et al. (2017)	$Min(H_c + D_c + S_c + P_c)$	LH		✓	
Liu & Zhang (2018)	$Min(S_c + H_c + P_c)$	Outer-approximation	✓	✓	
Current paper	$Min(H_c + S_c + A_c + O_c)$	GA			✓

“T: Two-level, M: Multi-level, Cap : Capacity, PC: Parts commonalities, NP: Number of disassembled products, R-MRP: Reverse-material requirements planning, D_c : Disassembly operation cost, P_c : Purchase cost of root, H_c : Holding cost, S_c : Setup cost, LP: Linear programming, DP: Dynamic programming, LS-RMRP: Lot-sizing-RMRP, CBSA: Constraint-based simulated annealing, Z_c : Purchase cost of parts, W_c : Waste cost, C_c : Start-up cost, L_c : Lost sales cost, O_c : Overload cost, A_c : Backlogging cost, LH: Lagrangian heuristics, EOQ: Economic order quantity, DP: Dynamic programming”.

70 In the last two decades, there has been a growing interest in developing methods and approaches to cope
71 with uncertainties in supply and production planning. In the field of reverse logistics, the existing literature
72 is very limited and has focused mainly on the uncertainty of demand and/or disassembly yield.

73 For the uncertainty of demand, [Barba-Gutiérrez & Adenso-Díaz \(2009\)](#) used trapezoidal distributions
74 to characterize the problem. For solving the DLSP, they suggested a fuzzy Reverse Materials Requirement
75 Planning (RMRP) algorithm. The authors determine the quantity of EoL products to be disassembled at
76 each period. Their fuzzy RMRP approach (F-RMPR) seems to perform better than the traditional RMRP
77 algorithm with a reduced inventory level. However, the proposed approach only seeks to satisfy component
78 demands. The authors neglected the optimization of costs related to the disassembly process whereas these
79 are an important element for companies. One year later, [Kim & Xirouchakis \(2010\)](#) studied the CDLSP
80 with a multi-period planning, two-level bill-of-material (BOM) and a multi-type EoL product. To solve this
81 problem, they developed a Lagrangian relaxation heuristic to minimize the sum of expected total cost which
82 is equal to the sum of inventory, setup and penalty costs for the unfulfilled item demands. The work of [Fang
83 et al. \(2017\)](#) studied the multi-period and multi-product stochastic problem for remanufacturing systems. In
84 order to solve the studied problem, the authors introduced a scenario-based approach, a multi-stage stochastic
85 MILP and a heuristic based on Lagrangian relaxation. The impact of the uncertainty of the demands on the
86 solution is analyzed by a sensitivity study of several scenarios.

87 The uncertainty of yield occurs when the difference between the quantities of items released and those
88 obtained after disassembly is random. [Inderfurth & Langella \(2006\)](#) considered a multi-type product with
89 parts commonality and solve the single period disassembly-to-order problem under random disassembly yield
90 (number of units of components obtained from disassembling one unit of parent item). To solve the considered
91 problem, they developed a heuristic to reduce the expected disposal, purchasing and disassembly operation
92 costs. In [Inderfurth et al. \(2015\)](#), the authors developed a mathematical model to illustrate the effect of
93 stochastic disassembly yield on stochastically proportional and binomial models. The results indicate that
94 presuming binomial yield is preferable to assuming proportional yield.

95 Few studies have been published on the uncertainty of demand and yield. [Liu & Zhang \(2018\)](#) formulated
96 the stochastic DLSP with these uncertainties as a mixed integer nonlinear programming and developed an
97 outer approximation-based solution algorithm to solve it. In that paper, the authors simultaneously use the
98 maximum and minimum values of both a uniform (for demand) and normal (for stochastic disassembly yield)
99 distribution to solve the DLSP.

100 As explained previously, variability in disassembly times is often observed during disassembly processes.
101 The related uncertainty is due to technical problems (absenteeism, limited disassembly capacity, etc.) and
102 economic conditions (availability of EoL products and variability of costs, etc.). As far as we know, there is
103 not much literature on disassembly planning under uncertainty of durations. Most studies have only focused
104 on deterministic environments. The aim of our research is to investigate stochastic CDLSP, and it outlines
105 a new approach to optimize order and disassembling policies.

106 **3. Problem statement and model formulation**

107 *3.1. Problem statement*

108 Let us take a close look at the disassembly planning of a two level disassembly system in which the EoL
 109 product is disassembled into several components. A graphical illustration of the two-level BOM, N compo-
 110 nents and single type of EoL product is given in Fig. 1. The customer’s component requirements are known
 111 over the planning horizon and should be delivered on predefined delivery dates. The number in brackets
 112 represents the disassembly yield or the number of components obtained by the disassembly operation of one
 113 unit of the EoL product. At the beginning of each period, a disassembly order for EoL product is made.
 114 In each period, we assume a limited disassembly time capacity. If this capacity is not sufficient to meet the
 115 component requirements in a given period t , an additional capacity can be added with a unit penalty cost
 116 u_t .

117

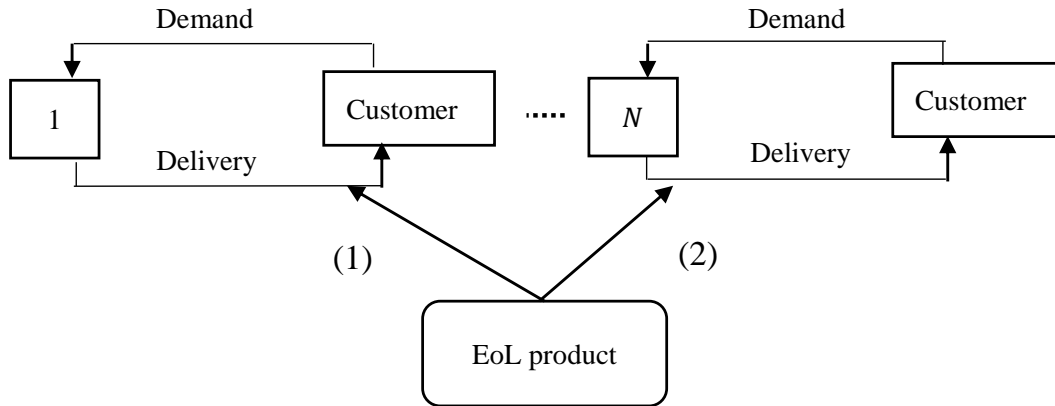


Figure 1: Two level disassembly system.

118 Disassembly systems are particularly vulnerable to EoL product disassembly lead times, since all the
 119 necessary components must be disassembled before the expected delivery dates. In fact, EoL product dis-
 120 assembly lead times, also named flow times, represent the time difference between releasing disassembly order
 121 and receiving the components from a disassembly order. To adhere more closely to industrial methods of
 122 planning, we assume a discrete temporal environment. The actual lead times are random discrete variables
 123 with known and finite possible values, and follow a known probability distribution. In fact, we assume that
 124 the workshop which disassembles the EoL products receives them from several disassembly lines. The work-
 125 load of these workshops varies from period to period. In this case, each disassembly lead time depends on
 126 the quality of the EoL product and the workload of the refurbishment workshop at each period t . Thereafter,
 127 the disassembled items are available after a stochastic disassembly lead time (L_t).

128

129 Before modeling the considered problem, we detail the following assumptions frequently encountered for
 130 this type of problem (Kim et al., 2006b, 2009; Kim & Xirouchakis, 2010):

- 131 • The end-of-life products are available once they are requested;
- 132 • Dynamic demands for the components are known over the planning horizon;
- 133 • Demands are only satisfied by the disassembly system;
- 134 • All disassembled items are in good condition to satisfy the demand;

135 As EoL disassembly lead times are random variables over the planning horizon, we provide a scenario
 136 based stochastic optimization formulation. A scenario represents a possible realization of the disassembly
 137 lead time in each period. More precisely, the lead times L_t are random discrete variables varying between L^-
 138 and L^+ . Thus, if any disassembly process starts in period t , all components are available at period $t + L_t$.
 139 Note that, if any disassembly order is released in period t , a setup cost s_t is occurred in that period. When
 140 a component i is received before its desired delivery date, an inventory holding cost h_i per period of time is
 141 incurred. Conversely, a backloging cost b_i is assessed at the end of each period per unit backloged. The
 142 objective is to optimize the disassembly quantities of the EoL product to minimise the sum of the expected
 143 holding and backlog costs of all disassembled components among all scenarios, as well as the setup and
 144 overload costs over a finite horizon.

145 3.2. Two-stage mixed integer linear programming (2S-MILP)

146 To solve the CDLSP with stochastic disassembly lead times, a stochastic 2S-MILP is proposed to minimize
 147 the expected total cost, denoted by $\mathbb{E}(TC)$, and to select the appropriate disassembly schedule plan i.e. the
 148 optimal quantity of EoL product to disassemble at each period over the planning horizon. The full list of
 149 notations used throughout this paper is given in Table 2.

150 **Definition 3.1.** Let Ω_0 be the set of all possible scenarios which contains all combinations of the random
 151 disassembly lead times. Each scenario ω corresponds to the realisations of all lead times of periods $1, \dots, t$.
 152 Its probability value is \mathbb{P}_ω . Knowing that all disassembly times are independent, so $\mathbb{P}_\omega = \prod_{t \in \mathcal{T}} \Pr(L_t = L_t^\omega)$
 153 and $|\Omega_0| = (L^+ - L^- + 1)^{|\mathcal{T}|}$.

Table 2: Notation.

Indexes	
t	index of periods, $\forall t = 1, \dots, T$
i	index of components, $\forall i = 1, \dots, N$
ω	index for scenarios, $\forall \omega = 1, \dots, \Omega_0 $
Parameters	
\mathcal{T}	set of time periods of the planning horizon , $ \mathcal{T} = T$
\mathcal{N}	set of components , $ \mathcal{N} = N$
Ω_0	set of possible scenarios

R_i	disassembly yield of component i
$D_{i,t}$	external demand for component i in period t
I_{i0}	starting inventory of component i
L_t^ω	disassembly lead time in period t for scenario ω
h_i	unit time inventory holding cost of one unit of component i
s_t	setup cost in period t
b_i	unit time backlog cost of one unit of component i
G	disassembly operation time
C_t	available capacity in period t
u_t	cost of adding a unit of extra capacity in period t
K	Large number

Functions

$\mathbb{E}(\cdot)$	Expected value
\mathbb{P}_ω	Probability value related to scenario ω , $\sum_{\omega \in \Omega} \mathbb{P}_\omega = 1$

First-stage decision variables

Z_t	disassembly quantity ordered in period t
Y_t	binary indicator of disassembly in period t
O_t	disassembly overtime in period t

Second-stage decision variables

H_{it}^ω	inventory level of component i at period t for scenario ω
B_{it}^ω	backlogging level of component i at period t for scenario ω
I_{it}^ω	inventory level at the end of period t . It is equal to $H_{it}^\omega - B_{it}^\omega$

154 The capacitated disassembly lot-sizing problem with stochastic disassembly lead times can be formulated
155 using the following stochastic 2S-MILP model based on scenarios formulation.

$$\mathbb{E}(TC) = \min \sum_{t \in \mathcal{T}} \left(\sum_{\forall i \in \mathcal{N}} \sum_{\omega \in \Omega_0} \mathbb{P}_\omega \left(h_i H_{i,t}^\omega + b_i B_{i,t}^\omega \right) + s_t Y_t + u_t O_t \right) \quad (1)$$

subject to constraints:

$$H_{i,t}^\omega - B_{i,t}^\omega = I_{i0} + \sum_{\tau \in \mathcal{T} \mid \tau + L_\tau^\omega \leq t} R_i Z_\tau - \sum_{\tau=1}^t D_{i,\tau} \quad \forall i \in \mathcal{N}, \forall t \in \mathcal{T}, \forall \omega \in \Omega_0 \quad (2)$$

$$Z_t \leq K \cdot Y_t \quad \forall t \in \mathcal{T} \quad (3)$$

$$G \cdot Z_t \leq C_t + O_t \quad \forall t \in \mathcal{T} \quad (4)$$

$$Z_t, O_t \geq 0 \quad \forall t \in \mathcal{T} \quad (5)$$

$$Y_t \in \{0, 1\} \quad \forall t \in \mathcal{T} \quad (6)$$

$$H_{i,t}^\omega, B_{i,t}^\omega \geq 0 \quad \forall i \in \mathcal{N}, \forall t \in \mathcal{T}, \forall \omega \in \Omega_0 \quad (7)$$

156 The $\mathbb{E}(TC)$ can be calculated by considering all possible values of L_t^ω and the objective function, expressed
 157 in Constraint (1) minimizes, for the first stage of the problem, the sum of the setup and penalty of extra
 158 capacity costs and the expected inventory holding and backlog costs for the second stage. Constraints (2)
 159 define for the second stage problem, the inventory balance for each component i at the end of each period t of
 160 scenario ω . Constraints (3) guarantee that a setup cost is generated in a period t if any disassembly operation
 161 needs to be performed in that period. Constraints (4) represent the disassembling capacity constraint in each
 162 period t . Constraints (5-6) provide the conditions framing the decision variables.

163 Before moving on to the core topic of this research, we briefly examine the complexity of the studied
 164 problem. According to Florian et al. (1980) and Bitran & Yanasse (1982), the single item capacitated lot-
 165 sizing problem (SCLSP) is a special case of the CDLSP with a single disassembled item and L_t equals to 0
 166 with probability 1. As the SCLSP is NP-hard, the CDLSP is NP-hard too.

167 4. Sample average approximation algorithm

168 Solving the 2S-MILP model with the set of all possible scenarios leads to the exact solution. However,
 169 the complexity of the problem may increase exponentially if a large set of Ω_0 is considered to represent the
 170 stochastic disassembly lead times and the proposed 2S-MILP becomes hard to solve. Therefore, in order
 171 to estimate the expected total cost (Kleywegt et al., 2002; Fishman, 1996), we propose the Sample Average
 172 Approximation (SAA) algorithm based on the Monte-Carlo (MC) sampling as proposed in Kim et al. (2018b).

173
 174 The flowchart of the SAA solution algorithm developed in this study is presented in Fig. 2. In this figure,
 175 Ω_1 , M and Ω_2 represent the current random sample size, the number of replications and the maximum sample
 176 size, respectively. The proposed algorithm includes three main steps at each replication: (1) generating Ω_1
 177 random scenarios for disassembly lead times; (2) solving the SAA problem and (3) checking the stopping
 178 condition (i.e. the variance of the gap estimator (VGE) and the percentage optimality gap (POG) must
 179 be sufficiently small). It is important to note that the three main steps are repeatedly carried out after the
 180 current random sample size Ω_1 is increased by a specified quantity ρ until the number of the random scenarios
 181 reaches the maximum Ω_2 unless the stopping condition is satisfied.

188 *4.2. Solving the sample average approximation problem*

Corollary 4.2. *For a given set of random samples L_t^ω for $\omega = 1, \dots, |\Omega_1|$, the SAA problem can be formulated as follow:*

$$ATC = \min \sum_{\forall t \in \mathcal{T}} \left(\sum_{\forall i \in \mathcal{N}} \sum_{\omega \in \Omega_1} \frac{1}{|\Omega_1|} \left(h_i H_{i,t}^\omega + b_i B_{i,t}^\omega \right) + s_t Y_t + u_t O_t \right) \quad (8)$$

subject to (3)-(6) and:

$$H_{i,t}^\omega - B_{i,t}^\omega = I_{i0} + \sum_{\tau \in \mathcal{T} \mid |\tau + L_i^\omega \leq t} R_i \cdot Z_\tau - \sum_{\tau=1}^t D_{i,\tau} \quad \forall i \in \mathcal{N}, \forall t \in \mathcal{T}, \forall \omega \in \Omega_1 \quad (9)$$

$$H_{i,t}^\omega, B_{i,t}^\omega \geq 0 \quad \forall i \in \mathcal{N}, \forall t \in \mathcal{T}, \forall \omega \in \Omega_1 \quad (10)$$

189 Expression (8) is an estimator of the expected total cost given in Expression (1). Constraints (9)-(10)
190 provide the inventory level for each component i at the end of each period t for each scenario $\omega \in \Omega_1$.

191 *4.3. Checking the stopping condition*

192 The third main step of the proposed SAA is to check the stopping condition. The proposed SAA algorithm
193 is stopped if the POG and the VGO are sufficiently small. These two parameters are estimated according to
194 the method proposed by Kleywegt et al. (2002) and Kim et al. (2018b).

195 *4.3.1. Estimation of the optimality gap*

The estimated optimality gap is the difference between the lower and the upper bounds. The lower bound
is calculated as the cumulative ATC from the first to the m^{th} replication as presented in Equation (11):

$$\overline{ATC}_{\Omega_1} = \frac{1}{m} \sum_{h=1}^m ATC_{\Omega_1}^h \quad (11)$$

196 where $ATC_{\Omega_1}^h$ represents the optimal ATC obtained at the h^{th} replication of the current sample size Ω_1
197 by solving the SAA problem. According to Mak et al. (1999); Norkin et al. (1998), $\overline{ATC}_{\Omega_1}$ gives a valid
198 statistical estimation of the lower bound because $\mathbb{E}(\overline{ATC}_{\Omega_1}) < \mathbb{E}(TC)$.

199

According to Kim et al. (2018b), any ATC obtained under Ω_2 sample size is always greater than or equal
to the $\mathbb{E}(TC)$. This is explained by the fact that ATC is an unbiased estimator of the objective function
value. Recall that Ω_2 is the maximum sample size that must be much greater than Ω_1 . Thus, an upper
bound ATC_{Ω_2} for a random sample of size Ω_2 can be estimated as presented in Equation (12):

$$ATC_{\Omega_2} = \min \sum_{\forall t \in \mathcal{T}} \left(\sum_{\forall i \in \mathcal{N}} \sum_{\omega \in \Omega_2} \frac{1}{|\Omega_2|} \left(h_i H_{i,t}^\omega + b_i B_{i,t}^\omega \right) + s_t Y_t + u_t O_t \right) \quad (12)$$

200 where $\{L_t^1, L_t^2, \dots, L_t^{\Omega_2}\}$ is the set of independent random scenarios of the disassembly lead time.

The percentage optimality gap (POG) can be calculated as follows:

$$POG = \left(\frac{ATC_{\Omega_2}^* - \overline{ATC}_{\Omega_1}}{ATC_{\Omega_1}} \right) \times 100$$

201 where $ATC_{\Omega_2}^*$ is the minimum ATC obtained over all the replications under Ω_2 random samples.

202 *4.3.2. Estimation of the variance gap estimator*

The variance gap estimator depends on the variances of $\overline{ATC}_{\Omega_1}$ and $ATC_{\Omega_2}^*$. It can be formulated as follows:

$$\sigma_{ATC_{\Omega_2}^* - \overline{ATC}_{\Omega_1}}^2 = \sigma_{ATC_{\Omega_2}^*}^2 + \sigma_{\overline{ATC}_{\Omega_1}}^2$$

where each of the two terms can be estimated as follow:

$$\sigma_{ATC_{\Omega_2}^*}^2 = \frac{1}{\Omega_2(\Omega_2 - 1)} \sum_{\omega=1}^{\Omega_2} \left(ATC_{\Omega_2} - ATC_{\Omega_2}^* \right)^2$$

and,

$$\sigma_{\overline{ATC}_{\Omega_1}}^2 = \frac{1}{m(m-1)} \sum_{h=1}^m \left(ATC_{\Omega_1}^h - \overline{ATC}_{\Omega_1} \right)^2$$

203 Although the SAA approach based on the MC simulation technique is interesting for estimating the expected
 204 total cost, it can suffer from the impossibility of obtaining optimal solutions as the complexity of the problem
 205 increases. An approximate solution method is needed to solve large problems. To study disassembly systems
 206 with more components and periods, introducing another resolution approach seems to be necessary.

207 **5. Genetic algorithm and Monte-Carlo simulation**

208 Various meta-heuristics are proposed in the literature to solve optimization problems. The genetic al-
 209 gorithm (GA) has a proven track record for the two-level assembly systems under random lead times (e.g.,
 210 Ben-Ammar et al., 2019, 2018; Guiras et al., 2019; Sakiani et al., 2012; Fallah-Jamshidi et al., 2011; Hnaïen
 211 et al., 2010, 2009). For this reason, we decided to use the GA to optimize the two-level disassembly systems
 212 studied in this research. In fact, the representation of the solutions and the reproduction operators (crossover
 213 and mutation) can easily be set up for the considered problem. Moreover, insofar as there are no particular
 214 constraints, meta-heuristics based on a local search, such as taboo search or simulated annealing, would
 215 require the exploration of a large number of neighbors and thus a significant computation time.

216 A genetic algorithm coupled with the Monte Carlo sampling (MC-GA) approach is suggested to calculate
 217 the quantity of EoL product to be disassembled in each period while minimizing the average total cost given
 218 in Equation (8). This approach is modeled and inspired by the natural evolutionary process (Goren et al.,
 219 2010) which is based on a randomly generated population of individuals. Given the important literature
 220 existing on the topic, for the objective of the present paper, it suffices to recall few basic notions regarding
 221 the GA technique. Fig. 3 shows a flowchart of the proposed MC-GA. The different steps will be presented,
 222 in detail, in the following sub-sections.

223 *5.1. Generation of the initial population of size n_{pop}*

224 In the implementation of an MC-GA, the first step is to create the initial population of individuals. Each
 225 individual is coded by a chromosome. The variables in the SAA model are $H_{i,t}^\omega$, $B_{i,t}^\omega$, O_t among $Z_t > 0$ if
 226 $Y_t=1$ and $Z_t=0$ otherwise, $\forall i \in \mathcal{N}, \forall t \in \mathcal{T}, \forall \omega \in \Omega_1$. In this study, we only encode Z_t the disassembly quantity

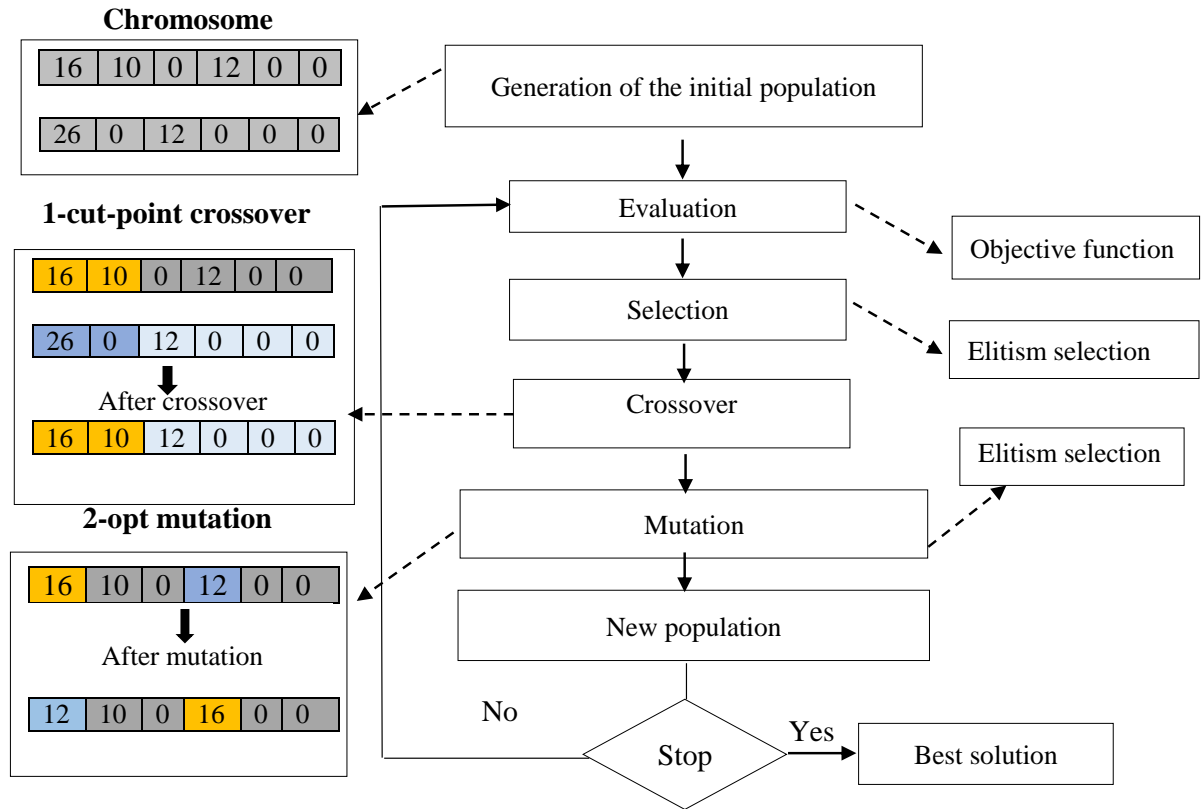


Figure 3: Flowchart of the proposed MC-GA.

227 of EoL product ordered in each period t . The other variables depend on Z_t and so they are not taken into
 228 account in the encoding step. Therefore, each gene in a chromosome represents a quantity of EoL product
 229 to be disassembled in each period t . The length of the chromosome is equal to the number of periods T . A
 230 Monte Carlo code must be run for each individual of the population throughout all the generations. Thus,
 231 each individual is built in many steps (see the procedure of generation of each individual of the population
 232 in Fig. 4).

233 **Step 1:** The first step is to generate the disassembly periods randomly ($Z_t > 0$ and $Y_t = 1$). Let $j < t$ to
 234 be the period such as $Z_j > 0$ and $Z_k = 0$, for $k = j + 1, \dots, t$. This implies that the amount of EoL product
 235 is the quantity needed to satisfy the demands of all components from the period j to t , such as $j \leq k \leq t$.
 236 We can see that the problem can be decomposed into t -period sub-problems (one of the periods j to t , and
 237 the other periods $t + 1$ to T). Let l_t be the last setup period in t -period sub-problem (i.e. t is the last setup
 238 period in t -period).

Step 2: The second step allows the calculation for each t -period, the disassembly quantity Z_j in period
 j . The exact value of Z_j is determined in order to satisfy the maximum demand among all the components

of the period j to t and all scenarios. We can determine Z_j using Equations (13) and take this lot-size plan as a final one. The main method of generating the GA is that the initial population is randomly generated. This method does not necessarily provide solutions that respect the disassembly capacity in each time period. Therefore, each overloading will be penalized.

$$Z_j = \max_{[\forall i, \forall \omega]} \left\lceil \frac{\sum_{i=1}^N \sum_{k=j}^t D_{i,k} - H_{i,j-1}^\omega + B_{i,j-1}^\omega}{R_i} \right\rceil \text{ and } Z_k = 0 \quad \forall k = j+1, \dots, t \quad (13)$$

239 where $\lceil x \rceil$ is the smallest integer greater than or equal to x .

The relation between the ordered and received quantities of disassembled EoL product is defined by Equations (14). Let $X_{t'}^\omega$ be the quantity of EoL products received at period t' for the scenario ω . Therefore, depending on the disassembly lead time, the scenario is that an order placed at period j will be received at $t' = j + L_j^\omega$. We underline that several orders made at different dates can be received at the same time. That explains why the received quantity is the sum of the orders having the same delivery date:

$$X_{t'}^\omega = \sum_{j \leq t'} Z_t, \quad \text{if } j + L_j^\omega = t' \quad \forall j, t' \in \mathcal{T}, \forall \omega \in \Omega_1 \quad (14)$$

Step 3: For each t -period, we can calculate the inventory and backlogging levels for each component i and scenario ω at the end of period k ($j \leq k \leq t$) by using Equations (15) and (16), respectively:

$$H_{i,k}^\omega = (H_{i,k-1}^\omega + R_i X_{t'}^\omega - D_{i,k} + B_{i,k-1}^\omega)^+ \quad \forall k = j, \dots, t \in \mathcal{T}, \forall \omega \in \Omega_1, \forall i \in \mathcal{N} \quad (15)$$

$$B_{i,k}^\omega = (H_{i,k-1}^\omega + R_i X_{t'}^\omega - D_{i,k} + B_{i,k-1}^\omega)^- \quad \forall k = j, \dots, t \in \mathcal{T}, \forall \omega \in \Omega_1, \forall i \in \mathcal{N} \quad (16)$$

240 where $(X)^+ = \max\{0, X\}$ and $(X)^- = \max\{0, -X\}$.

Step 4: After obtaining all the quantities of the EoL product to be ordered in each period t , we determine the additional capacity O_t using Equation (17) and then penalize its violation.

$$O_t = (G \times Z_t - C_t)^+ \quad \forall t \in \mathcal{T} \quad (17)$$

241 5.2. Evaluation

242 We use Equation (8) to evaluate the fitness value of each individual.

243 5.3. Selection

244 There are many selection methods in the literature such as rank selection, Elitist selection, Boltzmann
 245 selection, roulette selection, etc. (Belkhamisa et al., 2018). Based on the significant amount of literature related
 246 to replenishment planning under uncertainty of lead times where the Elitist selection is widely used (e.g.,
 247 Choi et al., 2009; Hnaïen et al., 2009; Che & Chiang, 2010), we decide to use this type of selection in this
 248 study. Thus, an individual is selected according to his performance. In our case, there are two selection
 249 phases:

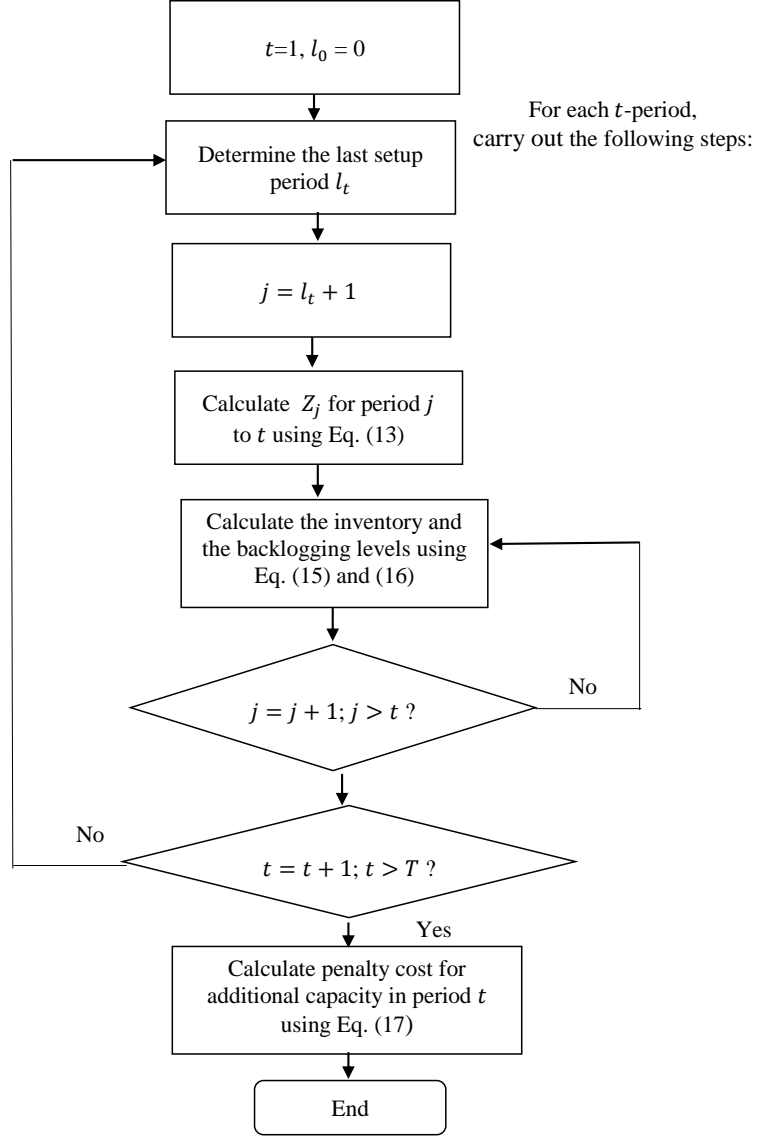


Figure 4: Procedure of generation of each individual.

- 250 • Reproductive selection: The $n_{pop}/2$ performed individuals in the population are chosen to undergo
 251 breeding operations (crossover and mutation). The selection is $n_{pop}/2$ Elitist.
- 252 • Replacement selection is the selection of each new population of at each generation. This new population
 253 is composed of the best individuals from the original generation and those obtained from mutation and
 254 crossover operations.

255 5.4. Crossover

256 The crossover operator permits us to produce a new individual called “offspring” from selected parents
 257 to obtain a “better” solution (Belkhamisa et al., 2018) (in our work, best quantity of the EoL product must
 258 be ordered in each period t). A standard 1-cut-point is considered. In this case, the first segment of the first

259 chromosome is followed by the second segment of the second chromosome (see 1-cut-point crossover in Fig. 3).
260 The crossover operator is performed according to a probability P_c . The cut-point is randomly generated.

261 5.5. Mutation

262 The mutation operator permits the diversification to be kept and to escape the local optima. It is a
263 matter of randomly modifying some individuals in our population by modifying one gene by another (see
264 2-opt mutation in Fig. 3). The mutation operator is performed according to a probability P_m .

265 5.6. New population

266 Once we have created new individuals by selection, crossover and mutation, we must select those who will
267 constitute the new population.

268 5.7. The stopping criteria

269 The GA process is repeated until the stopping criteria is met. The calculation time is an indispensable
270 factor in the decision making process. For this reason, as in Liu & Zhang (2018), we limit the computation
271 time to 600 seconds for the execution of the proposed approach.

272

273 In the next section, the proposed approaches are evaluated and several tests are performed to examine
274 the robustness of the solution approaches. We also examine the usefulness of the SAA and the MC-GA
275 approaches.

276 6. Computational experiments and results

277 In order to show the efficiency of the different solution methods, several numerical experiments were
278 performed. Three solution approaches are used to solve the studied problem. The first approach based on
279 the 2S-MILP model, gives exact solutions using all possible combinations of the random disassembly lead
280 times. The second approach based on the SAA algorithm, gives the average total cost based on random
281 sampling of the random parameter. The third approach is based on MC-GA. All tests are performed on a PC
282 with processor Intel (R) Core™ i7-5500 CPU @ 2.4 GHz and 8 Go RAM under Windows 10 Professional.
283 The two first approaches were solved by IBM CPLEX 12.6 within the fixed 3600 seconds time frame.

284 6.1. Numerical example

285 In this section we introduce a small numerical example. We considered a finite planning horizon with
286 7 periods and a two-level disassembly system with 3 components (1, 2 and 3) as shown in Fig. 5. The
287 disassembly operation extracts one component of type 1, two components of type 2 and one component of
288 type 3.

289 The demands for components over the planning horizon $D_{i,t}$ are listed in Table 4. The unit time inventory
290 holding and backlogging costs are $h_i=3$ and $b_i=100$, respectively $\forall i \in \mathcal{N}$. The setup cost s_t is equal to 20,

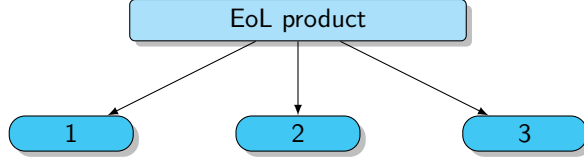


Figure 5: Two-level disassembly system

291 $\forall t \in \mathcal{T}$. Each disassembly lead time varies between 1 and 3 periods and follows the probability distribution
 292 given in Table 3. The disassembly operation time G is equal to 5. The available capacity C_t and the cost
 293 of adding a unit of extra capacity u_t are 80 and 10 $\forall t \in \mathcal{T}$, respectively. In this example, the number of all
 294 possible scenarios $|\Omega_0|$ is equal to $3^7 ((L^+ - L^- + 1)^{|\mathcal{T}|})$. In Table 4, we detail the optimal solution provided
 295 by the 2S-MILP model. More precisely, this table gives optimal values of variables in the two decision stages.
 296 In the first stage decision, we obtain the optimal quantity Z_t to be disassembled as well as the disassembly
 297 overtime O_t over the planning horizon. In the second stage decisions, the expected values of the inventory
 298 and the stockout of component i at each period t are calculated. The received quantities of component i at
 299 period t denoted by $\mathbb{E}(A_{i,t})$ are also presented in the same table. The optimal $\mathbb{E}(TC)$ takes the value 4752.43
 300 and is obtained in 65.12 seconds.

Table 3: Disassembly lead time probability distribution

l	1	2	3
$Pr(L_t = l)$	0.245	0.49	0.265

301

302 In order to test the convergence provided by the MC optimization approach, the numerical example was
 303 tested for different values of $|\Omega_1|$: [1, 30, 40, 50, 60, 70, 80, 90, 100, 200, ..., 1000]. Here we only applied the first
 304 two steps of the SAA algorithm, i.e. without checking the stopping condition or evaluating the quality of the
 305 solution. The number of replications was set to 10, i.e. $M = 10$ under a given sample size Ω_1 . Fig. 6 illustrates
 306 the convergence of the ATC (see Expression (8)) towards the exact value introduced in Expression (1) as
 307 well as the CPU needed to obtain this cost according to the different number of scenarios. On the one hand,
 308 this figure shows that the average total cost converges to the exact cost as the number of samples goes to
 309 infinity. In other words, a large number of samples is necessary to find a good approximation of the exact
 310 solution. On the other hand, for $\Omega_1 \geq 800$, the MC sampling provides a good approximation of optimal
 311 solution. Regarding the CPU, the same figure shows that the MC simulation-based approach can solve the
 312 problem in a reasonable time. Then, the application of the small test proved the effectiveness of the MC
 313 optimization approach that found a good compromise between the CPU time and the quality of the solution.

314 Fig. 6 describes how the optimal value ATC converges to $\mathbb{E}(TC)$ as the sample size Ω_1 increases. In the
 315 choice of sample size Ω_1 , the trade-off between the quality of an optimal solution of the SAA problem, and
 316 the bounds on the percentage optimality and the variance of gap estimator should be taken into account.

Table 4: Solution of the numerical example using the 2S-MILP model

Period t	1	2	3	4	5	6	7
Z_t	30	50	16	4			
O_t	70	170					
$D_{1,t}$				10	70	20	
$\mathbb{E}(H_{1,t})$		7.35	34.29	60.66	12.73		
$\mathbb{E}(B_{1,t})$						1.05	
$\mathbb{E}(A_{1,t})$		7.35	26.95	36.37	22.07	6.20	1.06
$D_{2,t}$				60	50		
$\mathbb{E}(H_{2,t})$		14.70	68.59	81.33	75.47	87.87	90.00
$\mathbb{E}(B_{2,t})$							
$\mathbb{E}(A_{2,t})$		14.70	53.90	72.70	44.18	12.40	2.12
$D_{3,t}$			10	20	50	20	
$\mathbb{E}(H_{3,t})$		7.35	26.30	40.66	12.73		
$\mathbb{E}(B_{3,t})$		2.00				1.05	
$\mathbb{E}(A_{3,t})$		7.35	26.95	36.37	22.11	6.16	1.06

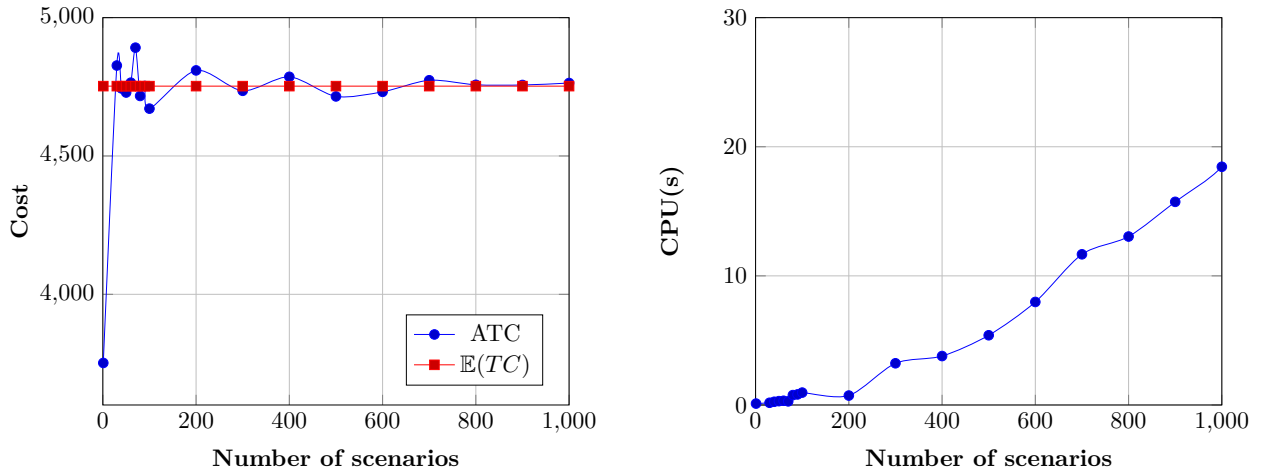


Figure 6: ATC convergence and CPU times.

317 In order to determine the random sample size that can be reached until a stopping condition is satisfied,
 318 a second test is performed and consists of applying the proposed SAA algorithm for different values of Ω_1 :
 319 $[1, 30, 40, 50, 60, 70, 80, 90, 100, 200, \dots, 1000]$. Recall that, if the percentage optimality and the variance of
 320 gap estimator are too large, the initial sample sizes Ω_1 must be increased until the sample size reaches the
 321 maximum Ω_2 unless the stopping condition is satisfied.

322 In our tests, the initial sample size is increased by 500 until the stopping condition is satisfied, i.e. the

percentage optimality gap and the variance of gap estimator for each replication are less than 5% and 10%, respectively. The maximum sample size $|\Omega_2|$ was set to 5,000. Fig. 7 shows the increased sample size as a function of the initial sample size. It can be seen from the figure that the increased sample size decreases as the initial sample size increases. In fact, the algorithm gave a robust solution with percentage optimality gap and variance of gap estimator less than 5% and 10%, respectively under the sample size of 1,000 without increasing the sample size.

The result of the SAA-based algorithm when the sample size Ω_1 was set to 1,000 is summarised in Table 5. It shows that the algorithm is stopped with the percentage optimality gap 4.02% and the variance of gap estimator 9.89% at the 5th replication. The resulting best quantities are $Z_1 = 30$, $Z_2 = 50$, $Z_3 = 20$, $Z_4 = 0$, $Z_5 = 0$, $Z_6 = 0$, $Z_7 = 0$. The related optimal *ATC* is equal to 4746 and obtained in only 19.92 seconds.

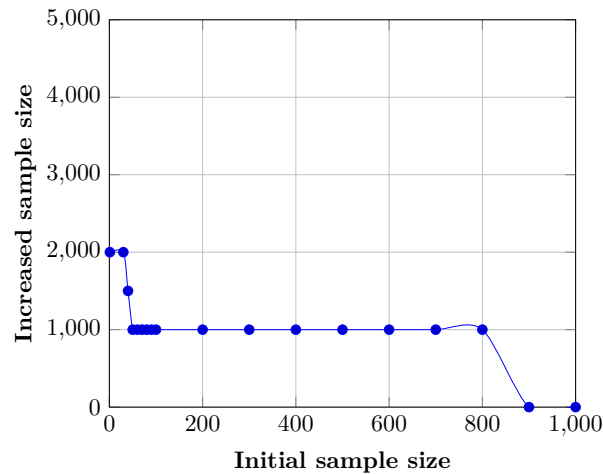


Figure 7: The increased random sample size as function of the initial random sample size.

332

333 6.2. Sensitivity analysis

334 In order to analyze the effect of disassembly lead times variability on the stability and robustness of the
 335 optimal solution found by the proposed SAA-based algorithm, the effect of variance (VAR) is treated. To do
 336 so, we generate 100 replications of the SAA problem under 1,000 random samples and we consider the same
 337 data instance presented in the previous sub-section. The probability distribution presented in Table 3 and
 338 denoted by VAR(a), is the reference case. Here, we vary the variance of the disassembly lead times between
 339 -75% and $+75\%$ as detailed in Table 6.

340 Fig. 8 illustrates the effect of the variation of the variance of disassembly lead times on the *ATC*. We
 341 firstly notice that, for a relatively low variation of the variance of disassembly lead times (VAR = -25%
 342 and $+25\%$), the variation of *ATC* increases slightly and remains at around $\pm 1\%$. For the large variationx
 343 ($\pm 75\%$), the variation of the *ATC* has also less significant impact on the average total cost and not exceed
 344 $\pm 3\%$. This proves that our approach remains robust even if the variance of lead times reaches $\pm 75\%$.

345

Table 5: SAA algorithm solution.

Replication (m)	Sample size ($\Omega_1 = 1,000$)	
	Percentage optimality gap	Variance of gap estimator (%)
1	4.12	-
2	6.23	19.24
3	4.54	11.75
4	5.77	09.15
5	4.02	09.89
6	-	-
7	-	-
8	-	-
9	-	-
10	-	-

Table 6: The changed distributions corresponding to different levels of VAR(a).

VAR	l	1	2	3
-75%	$\mathbb{P}(L_t = l)$	0.01	0.96	0.03
-50%	$\mathbb{P}(L_t = l)$	0.08	0.80	0.12
-25%	$\mathbb{P}(L_t = l)$	0.16	0.65	0.19
Var(a)	$\mathbb{P}(L_t = l)$	0.245	0.49	0.265
+25%	$\mathbb{P}(L_t = l)$	0.32	0.32	0.36
+50%	$\mathbb{P}(L_t = l)$	0.40	0.17	0.43
+75%	$\mathbb{P}(L_t = l)$	0.47	0.03	0.50

346 A second sensitivity analysis is provided to show the effects of capacity tightness, setup and backlog costs
347 by solving the SAA problem. Let β be a factor that can take value in the set $\{0.1, 0.5, 1.0, 5, 10\}$. In this
348 test, the capacity was generated from $\beta.C_t, \forall t \in \mathcal{T}$, the setup costs were generated from $\beta.s_t, \forall t \in \mathcal{T}$, and the
349 backlog costs were generated from $\beta.b_i, \forall i \in \mathcal{N}$. All other parameters are generated in the same manner in
350 section 6.1.

351 The test results are summarised in Table 7. The most remarkable result to emerge from the data is that
352 the amounts of setup and backlog costs do not show a particular trend on the effect on the gap. The average
353 percentage deviations were zero percent on average. Also, the amount of capacity and the setup costs affect
354 the computation time while the importance of backlog costs cannot be stressed for the SAA approach.

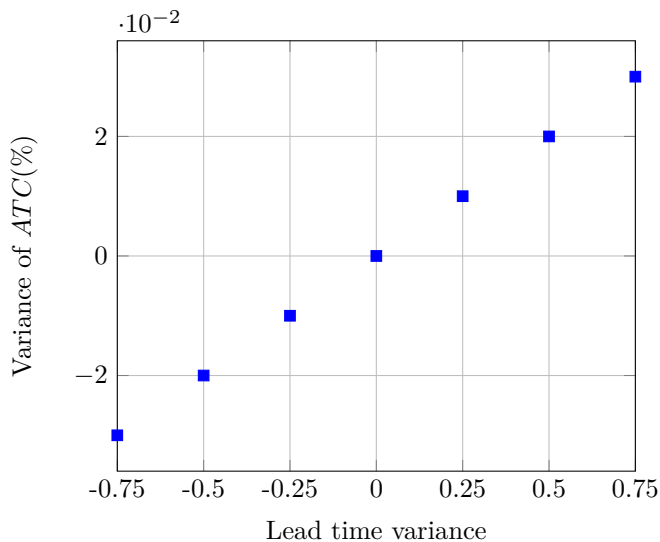


Figure 8: Effect of lead time variance on the expected total cost.

Table 7: Test results SAA approach.

Factor (β)	Capacity		Setup costs		Backlogging cost	
	Gap^*	CPU(s)	Gap^*	CPU(s)	Gap^*	CPU(s)
0.1	0.00	65.96	0.00	19.43	0.00	16.58
0.5	0.00	39.21	0.00	27.25	0.00	10.56
1	0.00	18.90	0.00	19.5	0.00	21.04
5	0.48	16.14	0.00	11.62	0.00	10.85
10	0.56	8.12	0.00	9.17	0.00	12.20
Mean	0.208	29.66	0.00	12.79	0.00	14.24

Gap^* : Percentage deviations from the lower bound or optimal solution value.

355 6.3. Random test instances

356 In order to compare and evaluate the 2S-MILP, SAA-based algorithm and MC-GA approaches more
 357 generally, the computational experiments involved different levels of problem size and complexity. The
 358 numerical examples are divided into two sets, where each set consists of several randomly generated problems.

359 The first set includes a disassembly system of 15 components. Since the problems in set 1 are small, they
 360 can be solved by all methods. Set 1 contains 3 different problems. The first one involves 10 time periods.
 361 The second one 20 time periods and the last one 30 time periods.

362 The second set consists of 5 problems of different sizes as presented in Table 8. Since, the problems in set
 363 2 are rather large, they are solved only by the MC-GA. For each problem, the disassembly lead times were
 364 taken as independent random variables. These variables are bounded by a known interval whose upper and
 365 lower limits are randomly generated and follow a discrete uniform distribution (see Table 8).

366 For each problem (set 1 and 2), the disassembly system is randomly generated. Without loss of generality

367 the initial inventory for all items was set to 0. All the tests are run under the data listed in Table 9. Here,
 368 $D \sim U(a, b)$ means that the parameter follows the discrete uniform distribution characterized by the interval
 369 $[a, b]$. In the previous sub-section, we showed that, with $\Omega_1 = 1,000$, a SAA approach can guarantee an almost
 370 exact solution for the stochastic problem. Accordingly, SAA-based algorithm and MC-GA approaches are
 371 used with a number of samples Ω_1 equal to 1,000.

Table 8: Characteristics of each problem in the second set.

Set	$[L^-, L^+]$	$ \mathcal{N} $	$ \mathcal{T} $
1	$D \sim U(1, 20)$	20	30
2	$D \sim U(1, 15)$	30	20
3	$D \sim U(1, 20)$	30	30
4	$D \sim U(1, 15)$	40	20
5	$D \sim U(1, 20)$	40	30

Table 9: Characteristics of data set.

Parameter	Value
$D_{i,t}$	$D \sim U(10, 100)$
h_i	$D \sim U(12, 20)$
s_t	$D \sim U(0, 1000)$
b_i	$2h_i$
u_t	$D \sim U(20, 25)$
R_i	$D \sim U(1, 5)$
C_t	$D \sim U(280, 480)$
G	$D \sim U(5, 15)$
$ \Omega_1 $	1,000

The good choice of the parameter values of the MC-GA makes a difference in the solutions' convergence. After preliminary tests, these parameters include the crossover rate ($P_c = 0.8$), the mutation rate ($P_m = 0.1$) and the population size ($n_{pop} = 200$ chromosomes). The average MC-GA solution cost convergence process for each problem (100 run of the MC-GA) for the first set, is shown in Fig. 9. The speed of convergence is determined by the size of the chromosomes and the number of generations. More especially, for the population whose chromosomes are 10 genes, we prolong the number of generations to 200 on average, to make sure that a near optimal solution is found. The best generation occurs at the 52nd generation as shown in Fig. 9(a). For chromosomes that contain 20 and 30 genes, better generation occurs on average at the 66th and 97th generations, respectively (see Fig. 9(b) and (c)). We prolong the end of generations to 250 and 400 for

problems 2 and 3 in set 1, respectively. For the following we define the gap between the best solution of the initial population ($bestSol_0$) and the best solution found after n generations ($bestSol_n$) using Equation (18).

$$gap = \frac{bestSol_0 - bestSol_n}{bestSol_n} \times 100 \quad (18)$$

372 The initial population seems to be of poor quality for each problem in set 1, which explains why the
 373 MC-GA gives an average improvement of 88 % during 200 generations on average for the first problem, 54.40
 374 % during 250 generations on average for the second problem and 67.89 % during 400 generations on average
 375 for the third problem in set 1. For the problems in set 2, we stopped the algorithm after 500 generations.
 376 We observed that the research space is sufficiently explored and that the population is rapidly evolving.

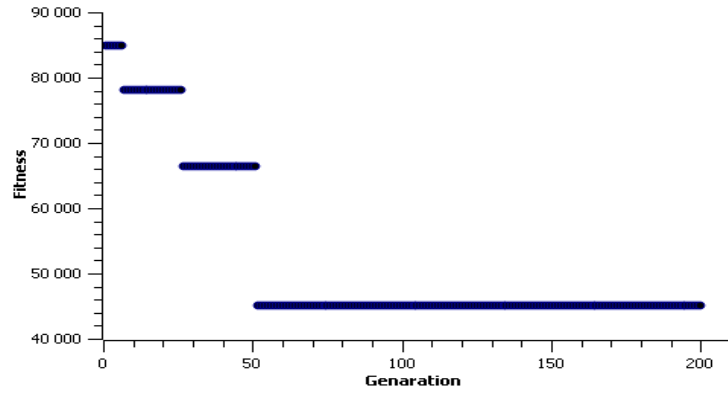
377 6.4. Effectiveness of the genetic algorithm approach

378 To validate the performance of MC-GA method, the test results are mentioned in this section. Recall
 379 that, we set the time limit as 3600(s) for the run of CPLEX in order to obtain the true optimal solution
 380 ($\mathbb{E}(CT)$) and the estimated optimal solution (ATC). For the GA execution, the computation time is limited
 381 to 600 seconds. In this case, we report the following performance measures throughout the numerical study:

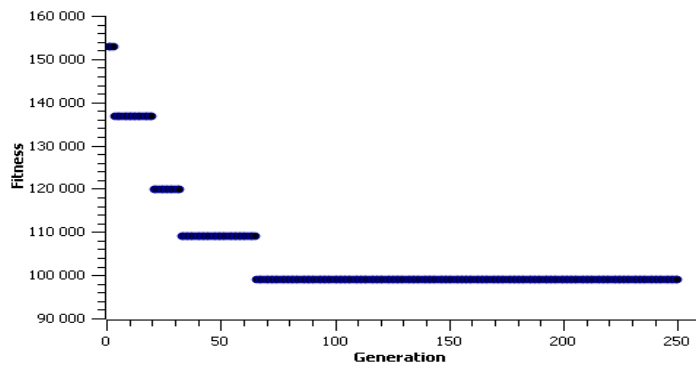
- 382 • the CPU time(s) needed to obtain optimal solutions;
- 383 • the integrality gap (G^*) given directly by CPLEX;
- 384 • the percentage deviation (G^+) between the average total cost (ATC) and the best solution given by
 385 the MC-GA ($bestSol_n$).
- 386 • the percentage deviation G^{++} between $ATC/or bestSol_n$ and the expected total cost ($\mathbb{E}(TC)$).

387 Table 10 presents the optimization results obtained by the 2S-MILP, SAA-based algorithm and MC-GA
 388 approaches, respectively for the problems of the first set (using the same data set). More precisely, this table
 389 gives the lead times range $[L^-, L^+]$, the computation time and the percentage deviations. In some cases, the
 390 results cannot be generated by the 2S-MILP model, which is indicated by a "-". Therefore, no comparison
 391 will be made, which is indicated by an "*".

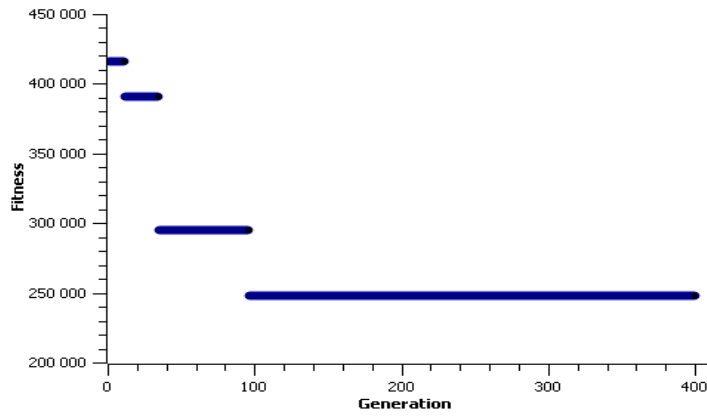
392
 393 Generally, we can observe that the 2S-MILP can only solve the problem with 10 periods when the dis-
 394 assembly lead time range does not exceed 1. This is due to the exponential number of possible scenarios
 395 which depends strongly on the number of periods. On the one hand, the SAA algorithm solutions presented
 396 in Table 10(b), indicate that the optimal disassembly schedule can be obtained within 3600 seconds using
 397 CPLEX until a disassembly system reaches 15 items and 30 periods. This is due to the fact that the capacity
 398 restrictions on disassembly resources and an increase in the number of periods and components, increase the
 399 problem size. On the other hand, the proposed MC-GA can solve a large problems by providing a satisfactory
 400 outcome in a short computational time. Given small deviations G^+ and G^{++} (less than 0.3% and 1.10%,



(a) Problem 1



(b) Problem 2



(c) Problem 3

Figure 9: Average MC-GA convergence for each problem in set 1.

401 respectively for all problems in set 1), the MC-GA plays an important role in finding a solution very close to
 402 the optimal one in a very reasonable time. In summary, this research successfully formulated and solved the
 403 CDLSP with random disassembly lead times.

404

Table 10: Performances of the MC-GA.

(a) 2S-MILP solutions for problems in set 1

Problem	$ \mathcal{N} $	$ \mathcal{T} $	$ \Omega $	$[L^-, L^+]$	CPU(s)	G^* (%)
1	15	10	2^{10}	[4,5]	675.22	0.00
2	15	20	15^{20}	[1,15]	-	-
3	15	30	20^{30}	[1,20]	-	-

(b) SAA approach solutions for problems in set 1

Problem	$ \mathcal{N} $	$ \mathcal{T} $	$ \Omega_1 $	$[L^-, L^+]$	CPU(s)	G^* (%)	G^{++} (%)
1	15	10	1,000	[4,5]	787.11	0.00	1.2
2	15	20	1,000	[1,15]	2615	0.00	*
3	15	30	1,000	[1,20]	3600	0.09	*

(c) MC-GA solutions for problems in set 1

Problem	$ \mathcal{N} $	$ \mathcal{T} $	$ \Omega_1 $	$[L^-, L^+]$	CPU(s)	G^+ (%)	G^{++} (%)
1	15	10	1,000	[4,5]	13.91	0.11	1.07
2	15	20	1,000	[1,15]	21.25	0.23	*
3	15	30	1,000	[1,20]	31.50	0.10	*

405 To show the effectiveness of the proposed MC-GA for large size tests, we deal with the second set of
 406 problems below. As explained previously, considering the random nature of the MC-GA, we carried out 100
 407 independent runs of the same data set of each problem in the second set. For each problem, the best and
 408 worst known solutions are selected. Subsequently, the gap between these two solutions noted $Gap_{w.run}^{b.run}$ is
 409 obtained as shown in Fig. 10. This figure clearly shows that the MC-GA results are stable. In fact, the total
 410 gap from the best to the worst run does not exceed 0.6 % for all problems in set 2.

411

412 As discussed in section 5.7, the CPU times required to obtain the best solutions is limited to 600(s).
 413 Fig. 11, shows that the proposed approach can solve a disassembly system of up to 40 components and 30
 414 periods. However, the number of periods has the most significant impact on the computation time.

415

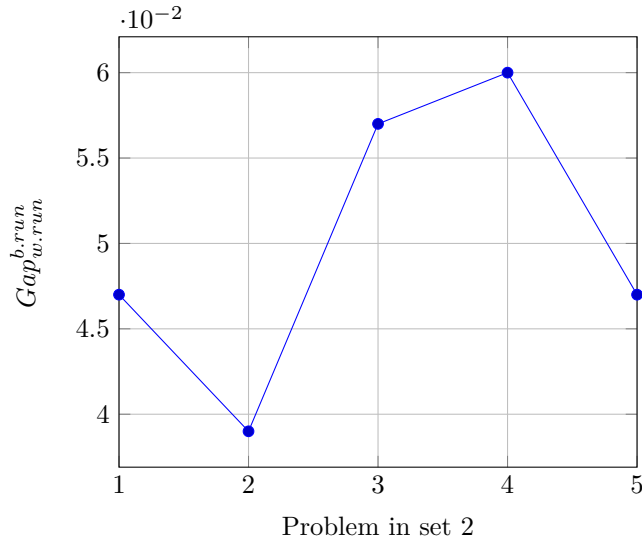


Figure 10: Average gap between the best and the worst run of each instance.

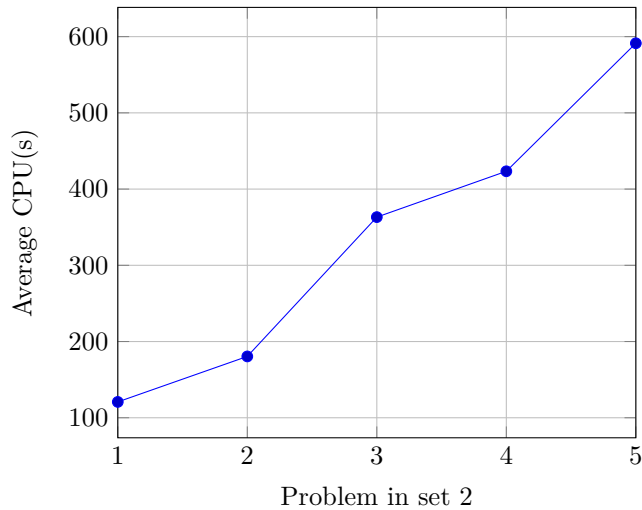


Figure 11: Average CPU(s) of each problem in set 2.

416 6.5. Managerial implications and insights

417 In reverse supply chain operation practice, disassembly lead time uncertainty is a common management
 418 issue. Guide Jr (2000) reported that the average disassembly and remanufacturing time of a typical recycled
 419 product can vary between 5.54 and 300 hours with coefficients of variation up to 5 hours. In that case, it is
 420 difficult to define the time required to complete the process of disassembling or obtaining the components.
 421 In this context, our study is unique in considering the uncertainty of disassembly lead time of the one type
 422 of end-of-life product and a two-level disassembly system in CDLSP.

423 The results presented in this paper reveal that a bad disassembly lead time management policy can be
 424 critical in disassembly systems. This type of uncertainty has a significant impact on the various costs of the
 425 disassembly process which will directly affect the overall operational performance of the reverse supply chain

426 especially in the case where the holding and the backlog costs are high.

427 In this study, we have used stochastic optimization models that take into account decisions to manage
428 this type of uncertainty and allow better control of it. The proposed models and methods can be applied by
429 decision makers to determine when and how many products should be disassembled to satisfy demand of all
430 leaf items and to minimize the generated costs.

431 From a practitioner's point of view, the interest of our approach lies in the fact that it can be used in
432 many industrial situations, as there are no assumptions on the cost functions and probability distributions
433 of the disassembly lead time. Moreover, the proposed model assures practitioners that even in the presence
434 of uncertainty in the DLT of an EoL product, the proposed approaches are tools that could help decision
435 makers cope with lead time uncertainties and plan disassembly operations in the most cost effective, easy
436 and efficient manner. However, with the availability of large amounts of data or dealing with large size
437 issues, optimization of disassembly processes could be done in real time. In this case, these models could
438 also be reinforced by techniques derived from Artificial Intelligence such as for example Machine learning,
439 data mining which will allow the extraction of probability distributions to guarantee the performance of the
440 models and methods proposed. In addition, a Digital twins concept and related approaches by collecting and
441 storing large amounts of data in real-time and throughout disassembly processes could be studied.

442

443 7. Conclusion

444 This paper addresses the capacitated disassembly lot-sizing problem under given demand and uncertain
445 disassembly lead times. The probability distribution of the disassembly lead time is assumed to be known
446 and bounded. The planning problem identifies how much EoL product to disassemble during each period in
447 order to minimize the expected total cost. Using a scenario-based approach to express stochastic disassembly
448 lead times, the considered problem is modelled as a two-stage stochastic Mixed-Integer Linear Program. To
449 alleviate the scalability issues, a sample average approximation-based solution algorithm is suggested. In
450 addition, to solve large scale problems, we propose a basic genetic algorithm. Experimental results show the
451 effectiveness of the proposed models and the convergence of the resulting Monte Carlo sampling. Finally,
452 based on our analysis, we have generated an important managerial implications

453

454 This paper could be extended in several ways. As for the lot-sizing (LS) perspective, most works treat the
455 problem under uncertainty on the two-level DLS problems. Since most of the real life, DLS are multi-levels. A
456 promising future research area could be solving the multi-level and multiple type of EoL product disassembly
457 system. For the GA perspective, the hybridization of the genetic algorithm with other meta-heuristics or
458 heuristic optimization techniques has caught the attention of many researchers in LS literature.

459

460 **References**

- 461 Agrawal, S., & Tiwari, M. (2008). A collaborative ant colony algorithm to stochastic mixed-model u-shaped
462 disassembly line balancing and sequencing problem. *International journal of production research*, *46*,
463 1405–1429.
- 464 Barba-Gutiérrez, Y., & Adenso-Díaz, B. (2009). Reverse mrp under uncertain and imprecise demand. *The*
465 *International Journal of Advanced Manufacturing Technology*, *40*, 413–424.
- 466 Barba-Gutiérrez, Y., Adenso-Díaz, B., & Gupta, S. M. (2008). Lot sizing in reverse mrp for scheduling
467 disassembly. *International Journal of Production Economics*, *111*, 741–751.
- 468 Belkhamza, M., Jarboui, B., & Masmoudi, M. (2018). Two metaheuristics for solving no-wait operating room
469 surgery scheduling problem under various resource constraints. *Computers & Industrial Engineering*, *126*,
470 494–506.
- 471 Ben-Ammar, O., Bettayeb, B., & Dolgui, A. (2019). Optimization of multi-period supply planning under
472 stochastic lead times and a dynamic demand. *International Journal of Production Economics*, *218*, 106–
473 117.
- 474 Ben-Ammar, O., Dolgui, A., & Wu, D. D. (2018). Planned lead times optimization for multi-level assembly
475 systems under uncertainties. *Omega*, *78*, 39–56.
- 476 Bitran, G. R., & Yanasse, H. H. (1982). Computational complexity of the capacitated lot size problem.
477 *Management Science*, *28*, 1174–1186.
- 478 Che, Z., & Chiang, C.-J. (2010). A modified pareto genetic algorithm for multi-objective build-to-order
479 supply chain planning with product assembly. *Advances in Engineering Software*, *41*, 1011–1022.
- 480 Choi, Y.-K., Lee, D. M., & Cho, Y. B. (2009). An approach to multi-criteria assembly sequence planning
481 using genetic algorithms. *The International Journal of Advanced Manufacturing Technology*, *42*, 180–188.
- 482 Dini, G., Failli, F., & Santochi, M. (2001). A disassembly planning software system for the optimization of
483 recycling processes. *Production Planning & Control*, *12*, 2–12.
- 484 Efendigil, T., Önüt, S., & Kongar, E. (2008). A holistic approach for selecting a third-party reverse logistics
485 provider in the presence of vagueness. *Computers & Industrial Engineering*, *54*, 269–287.
- 486 Fallah-Jamshidi, S., Karimi, N., & Zandieh, M. (2011). A hybrid multi-objective genetic algorithm for
487 planning order release date in two-level assembly system with random lead times. *Expert Systems with*
488 *Applications*, *38*, 13549–13554.
- 489 Fang, C., Liu, X., Pardalos, P. M., Long, J., Pei, J., & Zuo, C. (2017). A stochastic production planning
490 problem in hybrid manufacturing and remanufacturing systems with resource capacity planning. *Journal*
491 *of Global Optimization*, *68*, 851–878.

- 492 Fishman, G. (1996). Monte carlo: concepts, algorithms, and applications. *Science Business Media*, .
- 493 Florian, M., Lenstra, J. K., & Rinnooy Kan, A. (1980). Deterministic production planning: Algorithms and
494 complexity. *Management science*, *26*, 669–679.
- 495 Gao, N., & Chen, W. (2008). A genetic algorithm for disassembly scheduling with assembly product structure.
496 In *2008 IEEE International Conference on Service Operations and Logistics, and Informatics* (pp. 2238–
497 2243). IEEE volume 2.
- 498 Godichaud, M., & Amodeo, L. (2018). Economic order quantity for multistage disassembly systems. *Inter-
499 national Journal of Production Economics*, *199*, 16–25.
- 500 Godichaud, M., & Amodeo, L. (2019). Eoq inventory models for disassembly systems with disposal and lost
501 sales. *International Journal of Production Research*, *57*, 5685–5704.
- 502 Godichaud, M., Amodeo, L., & Hrouga, M. (2015). Metaheuristic based optimization for capacitated disas-
503 sembly lot sizing problem with lost sales. In *2015 International Conference on Industrial Engineering and
504 Systems Management (IESM)* (pp. 1329–1335). IEEE.
- 505 Goren, H. G., Tunali, S., & Jans, R. (2010). A review of applications of genetic algorithms in lot sizing.
506 *Journal of Intelligent Manufacturing*, *21*, 575–590.
- 507 Guide Jr, V. D. R. (2000). Production planning and control for remanufacturing: industry practice and
508 research needs. *Journal of operations Management*, *18*, 467–483.
- 509 Guiras, Z., Turki, S., Rezg, N., & Dolgui, A. (2019). Optimal maintenance plan for two-level assembly system
510 and risk study of machine failure. *International Journal of Production Research*, *57*, 2446–2463.
- 511 Gungor, A., & Gupta, S. M. (1998). Disassembly sequence planning for products with defective parts in
512 product recovery. *Computers & Industrial Engineering*, *35*, 161–164.
- 513 Güngör, A., & Gupta, S. M. (2001). Disassembly sequence plan generation using a branch-and-bound
514 algorithm. *International Journal of Production Research*, *39*, 481–509.
- 515 Gupta, S., & Taleb, K. (1994). Scheduling disassembly. *The International Journal of Production Research*,
516 *32*, 1857–1866.
- 517 Gupta, S. M., & Lambert, A. F. (2016). *Disassembly modeling for assembly, maintenance, reuse and recycling*.
518 CRC press.
- 519 Habibi, M. K. K., Battaïa, O., Cung, V.-D., Dolgui, A., & Tiwari, M. K. (2019). Sample average ap-
520 proximation for multi-vehicle collection–disassembly problem under uncertainty. *International Journal of
521 Production Research*, *57*, 2409–2428.

- 522 Han, H.-J., Yu, J.-M., & Lee, D.-H. (2013). Mathematical model and solution algorithms for selective
523 disassembly sequencing with multiple target components and sequence-dependent setups. *International*
524 *Journal of Production Research*, *51*, 4997–5010.
- 525 Hnaien, F., Delorme, X., & Dolgui, A. (2009). Genetic algorithm for supply planning in two-level assembly
526 systems with random lead times. *Engineering Applications of Artificial Intelligence*, *22*, 906–915.
- 527 Hnaien, F., Delorme, X., & Dolgui, A. (2010). Multi-objective optimization for inventory control in two-level
528 assembly systems under uncertainty of lead times. *Computers & operations research*, *37*, 1835–1843.
- 529 Ilgin, M. A., & Gupta, S. M. (2010). Environmentally conscious manufacturing and product recovery (ecm-
530 pro): A review of the state of the art. *Journal of environmental management*, *91*, 563–591.
- 531 Inderfurth, K., & Langella, I. M. (2006). Heuristics for solving disassemble-to-order problems with stochastic
532 yields. *OR Spectrum*, *28*, 73–99.
- 533 Inderfurth, K., Vogelgesang, S., & Langella, I. M. (2015). How yield process misspecification affects the
534 solution of disassemble-to-order problems. *International Journal of Production Economics*, *169*, 56–67.
- 535 Jeunet, J., Della Croce, F., & Salassa, F. (2019). Heuristic solution methods for the selective disassembly
536 sequencing problem under sequence-dependent costs. *IFAC-PapersOnLine*, *52*, 1908–1913.
- 537 Ji, X., Zhang, Z., Huang, S., & Li, L. (2016). Capacitated disassembly scheduling with parts commonality and
538 start-up cost and its industrial application. *International Journal of Production Research*, *54*, 1225–1243.
- 539 Kang, K.-W., Doh, H.-H., Park, J.-H., & Lee, D.-H. (2016). Disassembly leveling and lot sizing for multiple
540 product types: a basic model and its extension. *The International Journal of Advanced Manufacturing*
541 *Technology*, *82*, 1463–1473.
- 542 Kim, D.-H., Doh, H.-H., & Lee, D.-H. (2018a). Multi-period disassembly levelling and lot-sizing for multiple
543 product types with parts commonality. *Proceedings of the Institution of Mechanical Engineers, Part B:*
544 *Journal of Engineering Manufacture*, *232*, 867–878.
- 545 Kim, D.-H., & Lee, D.-H. (2011). A heuristic for multi-period disassembly leveling and scheduling. In *2011*
546 *IEEE/SICE international symposium on system integration (SII)* (pp. 762–767). IEEE.
- 547 Kim, H.-J., Lee, D.-H., & Xirouchakis, P. (2006a). A lagrangean heuristic algorithm for disassembly schedul-
548 ing with capacity constraints. *Journal of the Operational Research Society*, *57*, 1231–1240.
- 549 Kim, H.-J., Lee, D.-H., & Xirouchakis, P. (2006b). Two-phase heuristic for disassembly scheduling with
550 multiple product types and parts commonality. *International Journal of Production Research*, *44*, 195–
551 212.

- 552 Kim, H.-J., Lee, D.-H., & Xirouchakis, P. (2007). Disassembly scheduling: literature review and future
553 research directions. *International Journal of Production Research*, *45*, 4465–4484.
- 554 Kim, H.-J., Lee, D.-H., & Xirouchakis, P. (2008). An exact algorithm for two-level disassembly scheduling.
555 *Journal of the Korean Institute of Industrial Engineers*, *34*, 414–424.
- 556 Kim, H.-J., Lee, D.-H., Xirouchakis, P., & Kwon, O. (2009). A branch and bound algorithm for disassembly
557 scheduling with assembly product structure. *Journal of the Operational Research Society*, *60*, 419–430.
- 558 Kim, H.-J., Lee, D.-H., Xirouchakis, P., & Züst, R. (2003). Disassembly scheduling with multiple product
559 types. *CIRP Annals*, *52*, 403–406.
- 560 Kim, H.-J., & Xirouchakis, P. (2010). Capacitated disassembly scheduling with random demand. *International*
561 *Journal of Production Research*, *48*, 7177–7194.
- 562 Kim, H.-W., Park, C., & Lee, D.-H. (2018b). Selective disassembly sequencing with random operation times
563 in parallel disassembly environment. *International Journal of Production Research*, *56*, 7243–7257.
- 564 Kim, J.-G., Jeon, H.-B., Kim, H.-J., Lee, D.-H., & Xirouchakis, P. (2005). Capacitated disassembly schedul-
565 ing: minimizing the number of products disassembled. In *International Conference on Computational*
566 *Science and Its Applications* (pp. 538–547). Springer.
- 567 Kleywegt, A. J., Shapiro, A., & Homem-de Mello, T. (2002). The sample average approximation method for
568 stochastic discrete optimization. *SIAM Journal on Optimization*, *12*, 479–502.
- 569 Lamiri, M., Xie, X., Dolgui, A., & Grimaud, F. (2008). A stochastic model for operating room planning with
570 elective and emergency demand for surgery. *European Journal of Operational Research*, *185*, 1026–1037.
- 571 Langella, I. M. (2007). Heuristics for demand-driven disassembly planning. *Computers & Operations Re-*
572 *search*, *34*, 552–577.
- 573 Lee, D.-H., Kim, H., Choi, G., & Xirouchakis, P. (2004). Disassembly scheduling: integer programming mod-
574 els. *Proceedings of the Institution of Mechanical Engineers, Part B: Journal of Engineering Manufacture*,
575 *218*, 1357–1372.
- 576 Lee, D.-H., & Xirouchakis, P. (2004). A two-stage heuristic for disassembly scheduling with assembly product
577 structure. *Journal of the Operational Research Society*, *55*, 287–297.
- 578 Lee, D.-H., Xirouchakis, P., & Züst, R. (2002). Disassembly scheduling with capacity constraints. *CIRP*
579 *Annals*, *51*, 387–390.
- 580 Li, B., Ding, L., Rajai, M., Hu, D., & Zheng, S. (2018). Backtracking algorithm-based disassembly sequence
581 planning. *Procedia CIRP*, *69*, 932–937.

- 582 Li, K., Liu, Q., Xu, W., Liu, J., Zhou, Z., & Feng, H. (2019). Sequence planning considering human fatigue
583 for human-robot collaboration in disassembly. *Procedia CIRP*, *83*, 95–104.
- 584 Liu, J., Zhou, Z., Pham, D. T., Xu, W., Ji, C., & Liu, Q. (2020). Collaborative optimization of robotic
585 disassembly sequence planning and robotic disassembly line balancing problem using improved discrete
586 bees algorithm in remanufacturing. *Robotics and Computer-Integrated Manufacturing*, *61*, 101829.
- 587 Liu, K., & Zhang, Z.-H. (2018). Capacitated disassembly scheduling under stochastic yield and demand.
588 *European Journal of Operational Research*, *269*, 244–257.
- 589 Mak, W.-K., Morton, D. P., & Wood, R. K. (1999). Monte carlo bounding techniques for determining solution
590 quality in stochastic programs. *Operations research letters*, *24*, 47–56.
- 591 Neuendorf, K.-P., Lee, D.-H., Kiritsis, D., & Xirouchakis, P. (2001). Disassembly scheduling with parts
592 commonality using petri nets with timestamps. *Fundamenta Informaticae*, *47*, 295–306.
- 593 Norkin, V. I., Pflug, G. C., & Ruszczyński, A. (1998). A branch and bound method for stochastic global
594 optimization. *Mathematical programming*, *83*, 425–450.
- 595 Piewthongngam, K., Chatavithree, P., & Apichottanakul, A. (2019). Disassembly scheduling for the meat
596 processing industry with product perishability. *Journal of Advanced Manufacturing Systems*, *18*, 447–467.
- 597 Pour-Massahian-Tafti, M., Godichaud, M., & Amodeo, L. (2020a). Disassembly eoq models with price-
598 sensitive demands. *Applied Mathematical Modelling*, .
- 599 Pour-Massahian-Tafti, M., Godichaud, M., & Amodeo, L. (2020b). New models and efficient methods for
600 single-product disassembly lot-sizing problem with surplus inventory decisions. *International Journal of*
601 *Production Research*, (pp. 1–21).
- 602 Prakash, P., Ceglarek, D., & Tiwari, M. (2012). Constraint-based simulated annealing (cbsa) approach to
603 solve the disassembly scheduling problem. *The International Journal of Advanced Manufacturing Technol-*
604 *ogy*, *60*, 1125–1137.
- 605 Rai, R., Rai, V., Tiwari, M., & Allada, V. (2002). Disassembly sequence generation: a petri net based
606 heuristic approach. *International Journal of Production Research*, *40*, 3183–3198.
- 607 Ren, Y., Meng, L., Zhang, C., Zhao, F., Saif, U., Huang, A., Mendis, G. P., & Sutherland, J. W. (2020). An
608 efficient metaheuristics for a sequence-dependent disassembly planning. *Journal of Cleaner Production*,
609 *245*, 118644.
- 610 Sakiani, R., Ghomi, S. F., & Zandieh, M. (2012). Multi-objective supply planning for two-level assembly
611 systems with stochastic lead times. *Computers & Operations Research*, *39*, 1325–1332.

- 612 Slama, I., Ben-Ammar, O., Dolgui, A., & Masmoudi, F. (2020). New mixed integer approach to solve a
613 multi-level capacitated disassembly lot-sizing problem with defective items and backlogging. *Journal of*
614 *Manufacturing Systems*, 56, 50–57.
- 615 Slama, I., Ben-Ammar, O., Masmoudi, F., & Dolgui, A. (2019). Disassembly scheduling problem: literature
616 review and future research directions. *IFAC-PapersOnLine*, 52, 601–606.
- 617 Taleb, K. N., Gupta, S. M., & Brennan, L. (1997a). Disassembly of complex product structures with parts
618 and materials commonality. *Production Planning & Control*, 8, 255–269.
- 619 Taleb, K. N., Gupta, S. M., & Brennan, L. (1997b). Disassembly of complex product structures with parts
620 and materials commonality. *Production Planning & Control*, 8, 255–269.
- 621 Tian, X., & Zhang, Z.-H. (2019). Capacitated disassembly scheduling and pricing of returned products with
622 price-dependent yield. *Omega*, 84, 160–174.
- 623 Tiwari, M. (2005). Solving a disassembly line balancing problem with task failure using a psycho-clonal
624 algorithm. In *International Design Engineering Technical Conferences and Computers and Information in*
625 *Engineering Conference* (pp. 393–399). volume 47411.
- 626 Tseng, H.-E., Chang, C.-C., Lee, S.-C., & Huang, Y.-M. (2018). A block-based genetic algorithm for disas-
627 sembly sequence planning. *Expert Systems with Applications*, 96, 492–505.
- 628 Tseng, H.-E., Chang, C.-C., Lee, S.-C., & Huang, Y.-M. (2019). Hybrid bidirectional ant colony optimization
629 (hybrid baco): An algorithm for disassembly sequence planning. *Engineering Applications of Artificial*
630 *Intelligence*, 83, 45–56.
- 631 Ullerich, C., & Buscher, U. (2013). Flexible disassembly planning considering product conditions. *Interna-*
632 *tional Journal of Production Research*, 51, 6209–6228.
- 633 Xu, W., Tang, Q., Liu, J., Liu, Z., Zhou, Z., & Pham, D. T. (2020). Disassembly sequence planning
634 using discrete bees algorithm for human-robot collaboration in remanufacturing. *Robotics and Computer-*
635 *Integrated Manufacturing*, 62, 101860.
- 636 Zhang, X. F., & Zhang, S. Y. (2010). Product cooperative disassembly sequence planning based on branch-
637 and-bound algorithm. *The International Journal of Advanced Manufacturing Technology*, 51, 1139–1147.